Acta Crystallographica Section D
Biological Crystallography
ISSN 0907-4449

Purification, crystallization and preliminary X-ray analysis of the Fab fragment from MNAC13, a novel antagonistic anti-tyrosine kinase A receptor monoclonal antibody

Sonia Covaceuszach, Antonino Cattaneo and Doriano Lamba

Acta Crystallographica Section D
Biological Crystallography
ISSN 0907-4449

Purification, crystallization and preliminary X-ray analysis of the Fab fragment from MNAC13, a novel antagonistic anti-tyrosine kinase A receptor monoclonal antibody

Sonia Covaceuszach,[a] Antonino Cattaneo[a] and Doriano Lamba[b,c]*

[a]Neuroscience Program and Biophysics Unit Istituto Nazionale Fisica della Materia, International School for Advanced Studies, Via Beirut 2/4, I-34014 Trieste, Italy, [b]Istituto di Strutturistica Chimica 'G. Giacomello', Consiglio Nazionale delle Ricerche, Sez. di Trieste, Area Science Park, Basovizza, S.S 14 Km 163.5, I-34012 Trieste, Italy, and [c]International Centre for Genetic Engineering and Biotechnology, Area Science Park, Padriciano 99, I-34012 Trieste, Italy

Correspondence e-mail: lamba@sci.area.trieste.it

Received 19 April 2001
Accepted 26 June 2001

The monoclonal antibody MNAC13 is a potent antagonist that prevents the binding of nerve-growth factor (NGF) to its tyrosine kinase A receptor (TrkA) in a variety of systems. Structural studies of the FabMNAC13 fragment were performed to gain insights into the mechanism of action of this potentially therapeutic monoclonal antibody. The optimal conditions for crystallization of FabMNAC13 were determined. Crystals appeared as prismatic bundles, displayed $P2_12_12_1$ space-group symmetry and diffracted to a resolution of 1.8 Å. The unit-cell parameters were determined to be $a = 52.73$, $b = 67.55$, $c = 111.43$ Å. The data set was 99.5% complete. Molecular replacement was performed, resulting in a correlation coefficient of 0.55 and an R value of 0.40. The structure refinement is now in progress.

1. Introduction

TrkA is a transmembrane neurothrophin receptor with tyrosine kinase activity that shows high affinity towards NGF. This specific interaction promotes receptor dimerization, catalytic autophosphorylation of intracellular tyrosine residues and triggering of the signal transduction cascade (Kaplan & Stephens, 1994). These signals lead to prevention of apoptotic cell death (Maliartchouk *et al.*, 2000), promotion of cellular differentiation and axon elongation and up-regulation of choline acetyl transferase (Hefti *et al.*, 1985). It is worth noting that TrkA is expressed by several neuronal types, including sensory, sympathetic and cholinergic neurons which are implicated in important disease states. NGF is a potential therapeutic agent in the treatment of neurodegenerative diseases and nervous-system injuries (Cuello, 1996; Mufson *et al.*, 1997) as it promotes growth and survival of neurons during development and after neuronal damage. NGF antagonists would instead be useful in the treatment of certain chronic inflammatory or neuropathic pain states mediated by TrkA. Moreover, several human malignancies express normal TrkA and are NGF dependent or responsive; among them there are not only neuroectoderm-derived tumors such as medulloblastomas (Revoltella & Butler, 1980; Bauer *et al.*, 1992), neuroblastomas and glioblastomas (Oelmann *et al.*, 1995), but also non-neuronal carcinomas (Koizumi *et al.*, 1998) such as melanomas (Marchetti *et al.*, 1996), medullary thyroid carcinomas (Goretzki *et al.*, 1987; McGregor *et al.*, 1999), pancreatic carcinoid cell lines (Bold *et al.*, 1995) and prostate (Djakiew *et al.*, 1991), breast (Tagliabue *et al.*, 2000) and lung carcinomas.

The extracellular portion of TrkA is composed of five domains. The first three domains consist of a leucine-rich region and two cysteine-rich domains. The fourth and fifth domains (TrkA-d4 and TrkA-d5) are immunoglobulin (Ig) like domains. The TrkA-d5 domain adjacent to the membrane has previously been shown to be the dominant element for specific NGF binding (Perez *et al.*, 1995; Urfer *et al.*, 1995; Holden *et al.*, 1997). TrkA-d5 (Ultsch *et al.*, 1999; Robertson *et al.*, 2001) and its complex with NGF (Wiesmann *et al.*, 1999) have been crystallized and their structures elucidated. The structure of the TrkA-d5–NGF complex shows that the ligand–receptor interface consists of two patches: the first involves the central β-sheet that forms the core of the homodimeric NGF molecule and the loops at the carboxy-terminal pole of TrkA-d5. The second patch comprises the amino-terminal residues of NGF, which adopt a helical conformation upon complex formation, packing against the 'ABED' sheet of TrkA-d5. In the absence of complete structural information on the remaining four domains comprising the extracellular portion of TrkA, we sought an alternative approach to model the receptor–ligand interaction.

A novel antagonistic monoclonal antibody MNAC13 (Cattaneo *et al.*, 1999), raised against TrkA extra cellular domain, is known to block the interaction between NGF and TrkA in a variety of biological systems both *in vitro*

Table 1
Crystal parameters, data collection and processing statistics.

Values in parentheses are for the highest resolution shell.

Crystal	I	II
X-ray source	ELETTRA	ESRF
Wavelength (Å)	1.000	0.934
Detector	MAR 345	MAR CCD
Space group	$P2_12_12_1$	$P2_12_12_1$
Unit-cell parameters (Å)		
a	52.78	52.73
b	67.53	67.55
c	111.51	111.43
Mosaicity (°)	0.40	0.47
Resolution range (Å)	12.0–2.50 (2.59–2.50)	17.0–1.80 (1.83–1.80)
No. of measurements	98688	414115
No. of observed reflections, $I \geq 0$	56918	227914
No. of unique reflections, $I \geq 0$	14203 (1371)	38392 (1893)
Completeness (%)	99.5 (99.3)	99.5 (99.6)
Redundancy	4.0 (4.0)	5.9 (4.9)
$\langle I/\sigma(I)\rangle$ of measured data	9.4 (4.7)	8.2 (1.1)
$R_{\rm sym}$† (%)	5.7 (15.2)	6.3 (39.8)

† $R_{\rm sym}(I) = \sum_{hkl}\sum_i |I_{hkl,i} - \langle I_{hkl}\rangle|/\sum_{hkl}\sum_i |I_{hkl,i}|$, where $\langle I_{hkl}\rangle$ is the mean intensity of the multiple $I_{hkl,i}$.

(PC12) and *in vivo* (rat basal forebrain cholinergic neurons). The determination of its three-dimensional structure will provide deeper insight into the molecular basis of the observed high affinity of NGF for TrkA. Taken together, detailed structural information on the antigenic recognition by MNAC13 is expected to aid in the development of MNAC13 analogues as antagonists or agonists of neurotrophins that may have greater affinity or specificity for further experimental and therapeutic applications. As a first step into the mechanism of TrkA-NGF binding, we present here the purification, crystallization and preliminary X-ray analysis of the Fab fragment from this novel monoclonal antibody.

2. Experimental and results

2.1. Purification of the FabMNAC13

The MNAC13 hybridoma was prepared according to Cattaneo *et al.* (1999). The MNAC13 IgG1 immunoglobulin was purified from hybridoma supernatant by precipitation with 29% ammonium sulfate followed by affinity chromatography using a Protein G Sepharose column (Pharmacia) and eluted with low-pH buffer (10 m*M* HCl). MNAC13 IgG1 fractions were pooled and dialyzed across a Spectra-Por Membrane 12/14K (Spectrum) against 10 m*M* sodium phosphate pH 7.0, 20 m*M* EDTA. The MNAC13 IgG1 protein solution (10 mg ml^{-1}) was incubated with 13 m*M* Cys and treated with immobilized papain (Pierce) at an enzyme:substrate ratio of 1:15 for 5 h at 310 K. The resulting digest was dialyzed overnight against 100 m*M* Tris–HCl pH 8.0. The removal of Fc fragments was achieved by passage through a DEAE-Sephacel (Pharmacia) column equilibrated with the same buffer. FabMNAC13 was collected in the flowthrough, while Fc fragments and a fraction of uncleaved IgG1 were eluted with 200 m*M* NaCl. The Fab fragment was separated from the uncleaved IgG1 by size-exclusion chromatography on a Superdex G75 column (Pharmacia) equilibrated with 100 m*M* Tris–HCl pH 8.0, 150 m*M* NaCl. Fractions were assessed for homogeneity by Coomassie blue staining after separation by SDS–PAGE. The amounts of purified protein were determined by Lowry assay (Bio-Rad).

2.2. Crystallization

The purified FabMNAC13 fragment in 10 m*M* Tris pH 8.0 and 50 m*M* NaCl was concentrated to 5–10 mg ml^{-1} using Centricon 30K concentrators (Amicon). Initial crystallization experiments were based on the sparse-matrix sampling method (Jancarik & Kim, 1991) using Crystal Screens I and II purchased from Hampton Research (Laguna Niguel, CA, USA). All crystallization trials utilized the hanging-drop vapour-diffusion method and were conducted at 289 K. The best crystals were obtained mixing equal volumes (2 µl) of the protein stock solution with a reservoir solution (0.7 ml) containing 2 *M* ammonium sulfate, 5%(*v*/*v*) 2-propanol (Crystal Screen II, reagent No. 5). The resulting final pH was 7.5. Diffraction-quality crystals grew to their maximum dimensions in one week. A typical FabMNAC13 crystal is shown in Fig. 1.

2.3. Data collection

An initial X-ray diffraction data set was collected on an FabMNAC13 crystal (0.5 × 0.2 × 0.1 mm) using a MAR 345 imaging-plate detector (X-ray Research GmbH, Germany) at the XRD1 beamline of the ELETTRA synchrotron light source (Trieste, Italy). A higher resolution and more complete X-ray diffraction data set was collected on an FabMNAC13 crystal (0.8 × 0.3 × 0.2 mm) using a MAR CCD detector (MARUSA, USA) at the ID14-EH1 beamline, ESRF (Grenoble, France). The crystals were flash-cooled in liquid nitrogen at 100 K using an Oxford Cryosystems cooling device (Oxford, England) after a short soaking in a cryo-protectant solution containing 2.2 *M* ammonium sulfate, 6%(*v*/*v*) 2-propanol and 20%(*v*/*v*) glycerol. All X-ray diffraction data were indexed, integrated and subsequently scaled using the programs *DENZO* and *SCALEPACK* (Otwinowski & Minor, 1997), respectively; the *CCP*4 package (Collaborative Computational Project, Number 4, 1994) was used for data reduction. A summary and comparison of the X-ray diffraction data for the two crystals is given in Table 1. Assuming a molecular weight of 46 600 Da and one molecule in the asymmetric unit, the value of the crystal packing parameter $V_{\rm M}$ is 2.1 Å^3 Da^{-1}, corresponding to a solvent content of 42% (Matthews, 1968).

2.4. Phasing

Given that a number of crystal structures of Fab fragments are available, the most appropriate method for the determination of the FabMNAC13 structure was molecular replacement. A close scrutiny of the amino-acid sequence alignment of Fab fragments whose structures are present in the Protein Data Bank (Berman *et al.*, 2000) revealed that the most suitable model appeared to be 1bm3, the structure of an immunoglobulin Opg2 Fab–peptide complex (Kodandapani *et al.*, 1998). This Fab was chosen on the basis of sequence identity (70 and 88% for the heavy and light variable domains, respectively) and resolution (2.0 Å). The length of the CDRs matches the loop length in FabMNAC13 with the following exceptions: MNAC13_CDRL1 is shorter by one residue and MNAC13_CDRH3 is shorter by two residues. A preliminary model for the crystal structure of FabMNAC13 was obtained by molecular replacement using the program *AMoRe* (Navaza, 1994). It is well known that the so-called elbow angle of Fab molecules varies considerably between different

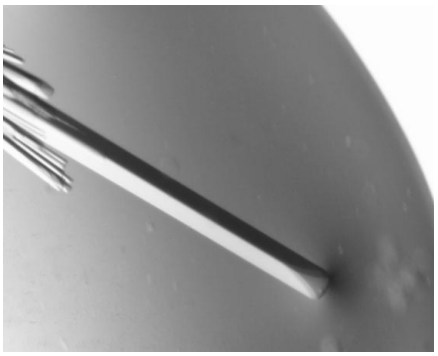

Figure 1
A typical prismatic bundle-like crystal of FabMNAC13, approximate dimensions are $0.8 \times 0.3 \times 0.2$ mm.

crystal structures. Therefore, the search model was divided into variable (V) and constant (C) domains; the V domains comprised residues 1–109 of the light chain and 1–125 of the heavy chain, while the C domains comprised the rest of the molecule (residues 110–214 of the light chain and 126–227 of the heavy chain). The cross-rotation function calculated with a Patterson integration radius of 32 Å using diffraction data in the resolution range 15.0–3.5 Å gave a distinct solution with a correlation coefficient (CC) of 0.21 for the V domains (0.14 for the next highest peak) and of 0.17 for the C domains (0.14 for the next highest peak). A translation function calculated for the space group $P2_12_12_1$ gave a clear solution for the V domains with a CC of 0.31 (0.24 for the next highest peak) and of 0.22 for the C domains (0.19 for the next highest peak). A two-body translation function was then calculated to confirm the consistency of the independent solutions for the variable and constant domains and to place these two components on a common crystallographic origin (CC of 0.45 and *R* factor of 0.44). Rigid-body refinement was subsequently performed to optimize the orientation and position of the two domains, resulting in a CC of 0.55 and an *R* factor of 0.40. The final model had structurally sensible pairing of the heavy and light variable domains with no steric obstruction to the packing of the Fab molecules in the unit cell, thus confirming the correctness of the solution. Current efforts are focused on model building and structure refinement using the high-resolution X-ray diffraction data set collected at the ESRF.

We are grateful to Società Italiana per la Ricerca Scientifica S.r.l for providing the MNAC13 hybridoma cell line from which the antibody was purified. We also thank Gabriella Rossi for her skilful technical assistance, and Kristian Vlahovicek, Jochen Wuerges and Kristina Djinovic Carugo for their assistance with data collection at the ELETTRA (Trieste, Italy) and the ESRF (Grenoble, France) synchrotron facilities.

References

Bauer, J., Margolis, M., Schreiner, C., Edgell, C.-J., Azizkhan, J., Lazarowski, E. & Juliano, R. L. (1992). *J. Cell. Physiol.* **153**, 437–449.
Berman, H. M., Westbrook, J., Feng, Z., Gilliland, G., Bhat, T. N., Weissig, H., Shindyalov, I. N. & Bourne, P. E. (2000). *Nucleic Acids Res.* **28**, 235–242.
Bold, R. J., Ishizuka, J., Rajaraman, S., Perez-Polo, R., Townsend, C. M. Jr & Thompson, J. C. (1995). *J. Neurochem.* **64**, 2622–2628.
Cattaneo, A., Capsoni, S., Margotti, E., Righi, M., Kontsekova, E., Pavlik, P., Filipcik, P. & Novak, M. (1999). *J. Neurosci.* **19**, 9687–9797.
Collaborative Computational Project, Number 4 (1994). *Acta Cryst.* D**50**, 760–763.
Cuello, A. C. (1996). *Prog. Brain Res.* **109**, 347–358.
Djakiew, D., Delsite, R., Pflug, B. R., Wrathall, J., Lynch, J. H. & Onoda, M. (1991). *Cancer Res.* **51**, 3304–3310.
Goretzki, P. E., Wahl, R. A., Becher, R., Koller, C., Branscheid, D., Grussendorf, M. & Roeher, H. D. (1987). *Surgery*, **102**, 1035–1042.
Hefti, F., Hartikka, J., Eckenstein, F., Gnahn, H., Heumann, R. & Schwab, M. (1985). *Neuroscience*, **14**, 55–68.
Holden, P. H., Asopa, V., Robertson, A. G., Clarke, A. R., Tyler, S., Bennett, G. S., Brain, S. D., Wilcock, G. K., Allen, S. J., Smith, S. K. & Dawbarn, D. (1997). *Nature Biotechnol.* **15**, 668–672.
Jancarik, J. & Kim, S.-H. (1991). *J. Appl. Cryst.* **24**, 409–411.
Kaplan, D. R. & Stephens, R. M. (1994). *J. Neurobiol.* **25**, 1404–1417.
Kodandapani, R., Veerapandian, L., Ni, C. Z., Chiou, C.-K., Whittal, R. M., Kunicki, T. J. & Ely, K. R. (1998). *Biochem. Biophys. Res. Commun.* **251**, 61–66.
Koizumi, H., Morita, M., Mikami, S., Shibayama, E. & Uchikoshi, T. (1998). *Pathol. Int.* **48**, 93–101.
McGregor, L. M., McCune, B. K., Graff, J. R., McDowell, P. R., Romans, K. E., Yancopoulos, G. D., Ball, D. W., Baylin, S. B. & Nelkin, B. D. (1999). *Proc. Natl Acad. Sci. USA*, **96**, 4540–4545.
Maliartchouk, S., Feng, Y., Ivanisevic, L., Debeir, T., Cuello, A. C., Burgess, K. & Saragovi, H. U. (2000). *Mol. Pharmacol.* **57**, 385–391.
Marchetti, D., McQuillan, D. J., Spohn, W. C., Carson, D. D. & Nicolson, G. L. (1996). *Cancer Res.* **56**, 2856–2863.
Matthews, B. W. (1968). *J. Mol. Biol.* **33**, 491–497.
Mufson, E. J., Lavine, N., Jaffar, S., Kordower, J. H., Quirion, R. & Saragovi, H. U. (1997). *Exp. Neurol.* **146**, 91–103.
Navaza, J. (1994). *Acta Cryst.* A**50**, 157–163.
Oelmann, E., Sreter, L., Schuller, I., Serve, H., Koenigsmann, M., Wiedenmann, B., Oberberg, D., Reufi, B., Thiel, E. & Berdel, W. E. (1995). *Cancer Res.* **55**, 2212–2219.
Otwinowski, Z. & Minor, W. (1997). *Methods Enzymol.* **276**, 307–326.
Perez, P., Coll, P. M., Hempstead, B. L., Martin-Zanca, D. & Chao, M. V. (1995). *Mol. Cell Neurosci.* **6**, 97–105.
Revoltella, R. P. & Butler, R. H. (1980). *J. Cell. Physiol.* **104**, 27–33.
Robertson, A. G. S., Banfield, M. J., Allen, S. J., Dando, J. A., Tyler, S. J., Bennett, G. S., Brain, S. D., Mason, G. G. F., Holden, P. H., Clarke, A. R., Naylor, R. L., Wilcock, G. K., Brady, R. L. & Dawbarn, D. (2001). *Biochem. Biophys. Res. Commun.* **282**, 131–141.
Tagliabue, E., Castiglioni, F., Ghirelli, C., Modugno, M., Asnaghi, L., Somenzi, G., Melani, C. & Menard, S. (2000). *J. Biol. Chem.* **275**, 5388–5394.
Ultsch, M. H., Wiesmann, C., Simmons, L. C., Heinrich, J., Yang, M., Reilly, D., Bass, S. H. & de Vos, A. M. (1999). *J. Mol. Biol.* **290**, 149–159.
Urfer, R., Tsoulfas, P., O'Connell, L., Shelton, D. L., Parada, L. F. & Presta, L. G. (1995). *EMBO J.* **14**, 2795–2805.
Wiesmann, C., Ultsch, M. H., Bass, S. H. & de Vos, A. M. (1999). *Nature (London)*, **401**, 184–188.